Heliyon

ELSEVIER

Received:
23 June 2016
Revised:
19 October 2016
Accepted:
11 November 2016

Heliyon 2 (2016) e00197

Heterogeneous regulation of bacterial natural product biosynthesis via a novel transcription factor

Antje K. Heinrich [a,1], **Angela Glaeser** [b,1], **Nicholas J. Tobias** [a], **Ralf Heermann** [b,*], **Helge B. Bode** [a,c,*]

[a] *Fachbereich Biowissenschaften, Merck Stiftungsprofessur für Molekulare Biotechnologie, Goethe-Universität Frankfurt, Frankfurt am Main, Germany*

[b] *Bereich Mikrobiologie, Biozentrum Martinsried, Ludwig-Maximilians-Universität München, München, Germany*

[c] *Buchmann Institute for Molecular Life Sciences (BMLS), Goethe-Universität Frankfurt, Frankfurt am Main, Germany*

* Corresponding authors.

E-mail addresses: heermann@lmu.de (R. Heermann), h.bode@bio.uni-frankfurt.de (H.B. Bode).

[1] Equal contribution.

Abstract

Biological diversity arises among genetically equal subpopulations in the same environment, a phenomenon called phenotypic heterogeneity. The life cycle of the enteric bacterium *Photorhabdus luminescens* involves a symbiotic interaction with nematodes as well as a pathogenic association with insect larvae. *P. luminescens* exists in two distinct phenotypic forms designated as primary (1°) and secondary (2°). In contrast to 1° cells, 2° cells are non-pigmented due to the absence of natural compounds, especially anthraquinones (AQs). We identified a novel type of transcriptional regulator, AntJ, which activates expression of the *antA-I* operon responsible for AQ production. AntJ heterogeneously activates the AQ production in single *P. luminescens* 1° cells, and blocks AQ production in 2° cells. AntJ contains a proposed ligand-binding WYL-domain, which is widespread among bacteria. AntJ is one of the rare examples of regulators that mediate heterogeneous gene expression by altering activity rather than copy number in single cells.

Keywords: Cell biology, Microbiology, Genetics

http://dx.doi.org/10.1016/j.heliyon.2016.e00197

1. Introduction

Phenotypic heterogeneity has recently developed into a major research focus in microbiology. Formerly, it was thought that genetically isogenic bacterial cell cultures coordinate gene expression collectively in a homogeneous environment. However, more and more examples arise showing that bacterial populations consist of genetically identical individual cells shaping different phenotypes, e.g. sporulation [1], bacterial competence [2], antibiotic production [3], or quorum sensing (see [4] for review). However, information about regulation mechanisms of bacterial phenotypic heterogeneity at the molecular level is rare to date.

Photorhabdus luminescens is an insect pathogenic enteric bacterium that maintains a mutualistic interaction with heterorhabditid nematodes, and can infect a variety of insect species. The bacteria colonize the gut of the infective juvenile stage (IJs) of the nematode *Heterorhabditis bacteriophora*. Upon entering insect larvae, the IJs release the bacteria by regurgitation directly into the insect's hemocoel. Once inside, the bacteria rapidly replicate and quickly establish a lethal septicaemia in the host by production of a broad range of different toxins that kill the insect within two days. Bioconversion of the insect's body by *P. luminescens* produces a rich food source for the bacteria as well as for the nematodes. The bacteria support nematode development and reproduction, probably by providing essential nutrients that are required for efficient nematode proliferation [5, 6]. Furthermore, the bacteria produce several antibiotics to defend the insect cadaver from other bacteria. When the insect cadaver is depleted, the IJs and bacteria re-associate and emerge from the carcass in search of a new insect host (see [7, 8] for overview).

P. luminescens is an ideal candidate to study phenotypic heterogeneity since the bacteria exist in two distinct phenotypically different forms, primary (1°) and secondary (2°) cells. During prolonged cultivation in insects or in culture medium, individual 1° cells switch to the 2° phenotype, so that in the end of the infection cycle approximately 20–50% of the cells have undergone the switching process [9, 10]. Both phenotypic variants are equally virulent towards insects. However, only 1° cells are known to associate with the nematodes and to trigger their development. Furthermore, 2° cells are unable to support nematode growth and development both in the insect cadaver as well as in culture. The reason why single cells of *P. luminescens* undergo phenotypic switching is not understood. It is assumed that the 2° variant is better adapted for a life in the soil, after being left in the insect cadaver while the 1° cells have emerged with the nematodes [11]. Evidently, 1° cells exhibit several phenotypic characteristics that are absent from 2° cells [9, 10]. One of the most distinct phenotypes of phenotypic heterogeneity in *P. luminescens* is pigmentation, which only occurs in 1° cells. Pigmentation is a result of the production of anthraquinones (AQ) (Fig. 1A). Among the natural products of *P. luminescens*, AQs have been extensively studied. AQs in general are

http://dx.doi.org/10.1016/j.heliyon.2016.e00197

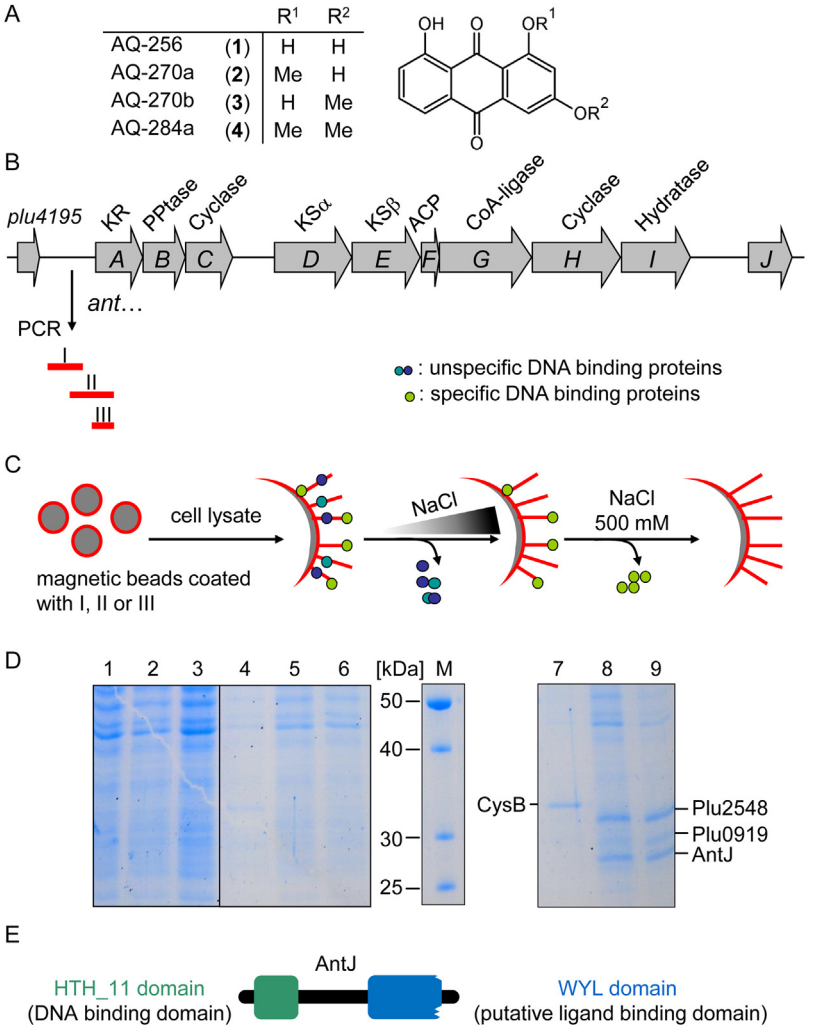

Fig. 1. AQ production of *P. luminescens* and schematic representation of the identification of unknown transcriptional regulators of the *antA-I* biosynthesis gene cluster via DNA protein pull down assay. **A.** Major AQs (**1**–**4**) produced by *P. luminescens*. **B.** Organization of the *ant* biosynthesis gene cluster of *P. luminescens* [14]. The promoter region of *antA* was amplified via PCR using 5′biotinylated forward primers yielding three overlapping, biotinylated DNA fragments (I–III). **C.** Immobilization of the DNA fragments I (internal control), II or III on streptavidin-coupled magnetic beads. Following incubation with cell lysate loose binding proteins were washed off by four washing steps with increasing NaCl concentrations. Finally, specific binding proteins were eluted in presence of 500 mM NaCl. **D.** SDS-PAGE, separated proteins of the DNA protein pull down assay. Coomassie blue stained polyacrylamide gel. 1–3: washing step 3 (175 mM NaCl) of fragments I–III, 4–6: washing step 4 (200 mM NaCl) of fragments I–III and 7–9: elution fraction (500 mM NaCl) of fragments I–III, M: protein marker. Protein bands smaller than 40 kDa and only visible in the elution fraction were cut out and identified via peptide mass fingerprinting. **E.** Domain structure of AntJ. The protein consists of two domains, an N-terminal HTH_11 domain, which is a putative DNA binding domain, and a C-terminal WYL domain, which is supposed to bind ligands [20].

http://dx.doi.org/10.1016/j.heliyon.2016.e00197

common in plants, fungi and streptomycetes, but *Photorhabdus* is the only known Gram-negative AQ producer [12, 13, 14]. The biosynthetic gene cluster (BGC) for AQ production (*antA-I*) encodes a type II polyketide synthase (PKS), namely AntD (KSα), AntE (KSβ) and AntF (ACP), as well as modifying enzymes (AntG-I) [14]. For some AQs weak antimicrobial activity was detected and they are assumed to play an ecological role serving as deterrents against birds and scavenger insects [11, 15, 16]. The exact physiological role of the AQs has yet to be elucidated. The mechanism of regulation of the heterogeneous pigmentation phenotype, and therefore AQ production, was similarly unknown.

Here we describe the identification of a regulator named AntJ that activates expression of the *antA-I* operon. AntJ is a novel type of regulator, harboring a putative DNA-binding domain that is essential for activation of AQ biosynthesis in *P. luminescens* 1° cells. The AQ promoter P_{antA} is heterogeneously activated in 1° cells, whereas there is also a basal but homogeneous P_{antA} activity present in 2° cells, although 2° cells do not exhibit AQ biosynthesis. Drastic overproduction of AntJ caused a homogeneous, strongly activated P_{antA} activity in 1° as well as in 2° cells and led to AQ production by the usually non-pigmented 2° cells. Since both 1° and 2° cells contained comparable levels of the regulator AntJ, we suppose that AntJ directly mediates heterogeneous expression of *antA-I* by adjusting its activity rather than its copy number.

2. Results

2.1. Identification of AntJ as transcriptional activator of the AQ biosynthesis gene cluster

In order to identify a putative regulator of the AQ biosynthesis operon *antA-I*, we performed a DNA-protein pull down assay using the upstream region of *antA*. First, the 986 bp region upstream of *antA* (P_{antA}) was subdivided into overlapping fragments (Fig. 1B, I–III), which were then immobilized on magnetic beads. Subsequently, the magnetic beads were incubated with *P. luminescens* 1° cell lysate and proteins binding to P_{antA} were pulled out and identified by peptide mass fingerprinting (PMF) (Fig. 1C, D). Overall, we identified several proteins that specifically bound to P_{antA}. The protein binding to fragment I (control) was identified as Plu2434 (CysB). In *E. coli* CysB is known to be a LysR-type family transcriptional regulator which positively regulates the cysteine regulon [17]. Three proteins corresponding to the bands between 40 and 25 kDa could be found in the elution fraction of fragment II as well as in the elution fraction of fragment III. Therefore, fragment III, a smaller internal fragment of II, must comprise the protein binding sites of the three proteins. The largest protein was identified as Plu2548, the intermediate protein band emerged as Plu0919 and the lowest band

http://dx.doi.org/10.1016/j.heliyon.2016.e00197

was determined to be Plu4185. The corresponding gene *plu4185* mapped directly adjacent to *antA-I* and therefore was renamed as *antJ*.

Plu2548 was annotated as LysR-type family transcriptional regulator, and Plu0919 was identified as one of 35 PAS4-LuxR-type transcriptional regulators, whose putative function in *P. luminescens* has been discussed before [18, 19]. AntJ consists of an N-terminal HTH_11 domain (PF08279) and a C-terminal truncated WYL-domain (PF13280) and shows weak similarity to the DNA binding transcriptional regulator YafY (COG2378) [20] (Fig. 1E).

Due to the fact that all identified proteins are putative DNA binding transcriptional factors, their function in regulation of the AQ biosynthesis was analyzed further. Therefore, the corresponding genes were deleted separately. Neither the deletion of *plu0919* nor of *plu2548* caused an altered pigmentation phenotype (Fig. S1). However, the deletion of *plu4185* (*antJ)* led to a complete loss of AQ production (Fig. 2A, c).

In order to elucidate the function of AntJ, we first examined the domain architecture. To date (October, 2016) the Pfam database counts 4519 protein sequences containing a predicted WYL-domain (PF13280) from 1659 different species. Nearly half of the proteins (2171) possess the same domain architecture as AntJ (N-terminal HTH_11 domain and C-terminal WYL-domain) including transcriptional regulators of human pathogens such as *Pseudomonas aeruginosa*. A phylogenetic tree, which includes the closest homologues of AntJ (based on blastp analyses), demonstrates that AntJ is only distantly related to its closest homologues (Fig. 3 and Table S5). AntJ also shows a low sequence identity to the predicted HTH_11/WYL regulators of the closely related genus *Xenorhabdus* (e.g. 44–43% sequence identity for orthologous HTH_11/WYL regulators from *Xenorhabdus doucetiae, Xenorhabdus nematophila*, *Xenorhabdus szentirmaii, Xenorhabdus bovienii*) (NCBI blastp). *Photorhabdus temperata*, another AQ producer contains an AntJ homologue with 91% sequence identity (NCBI blastp). The corresponding gene similarly maps directly downstream of the predicted AQ biosynthesis gene cluster. *Photorhabdus asymbiotica* does not produce AQs [21], and we could not detect any AntJ homologue in this species.

2.2. AntJ positively regulates AQ production

In order to investigate a putative role of AntJ in the AQ biosynthesis, a marker-less deletion of the *antJ* gene in 1° cells was generated, yielding the strain TT01−1°Δ*antJ*. TT01–1° colonies as well as the liquid culture have an orange-red color as a result of AQ production. In contrast, TT01−1°Δ*antJ* colonies are beige to weak yellowish and the liquid culture is non-pigmented. HPLC-UV confirmed that the *antJ* deletion strain no longer produces any AQs (Fig. 2A, c). Complementation of Δ*antJ* was achieved *in trans* by introducing a low-copy

http://dx.doi.org/10.1016/j.heliyon.2016.e00197

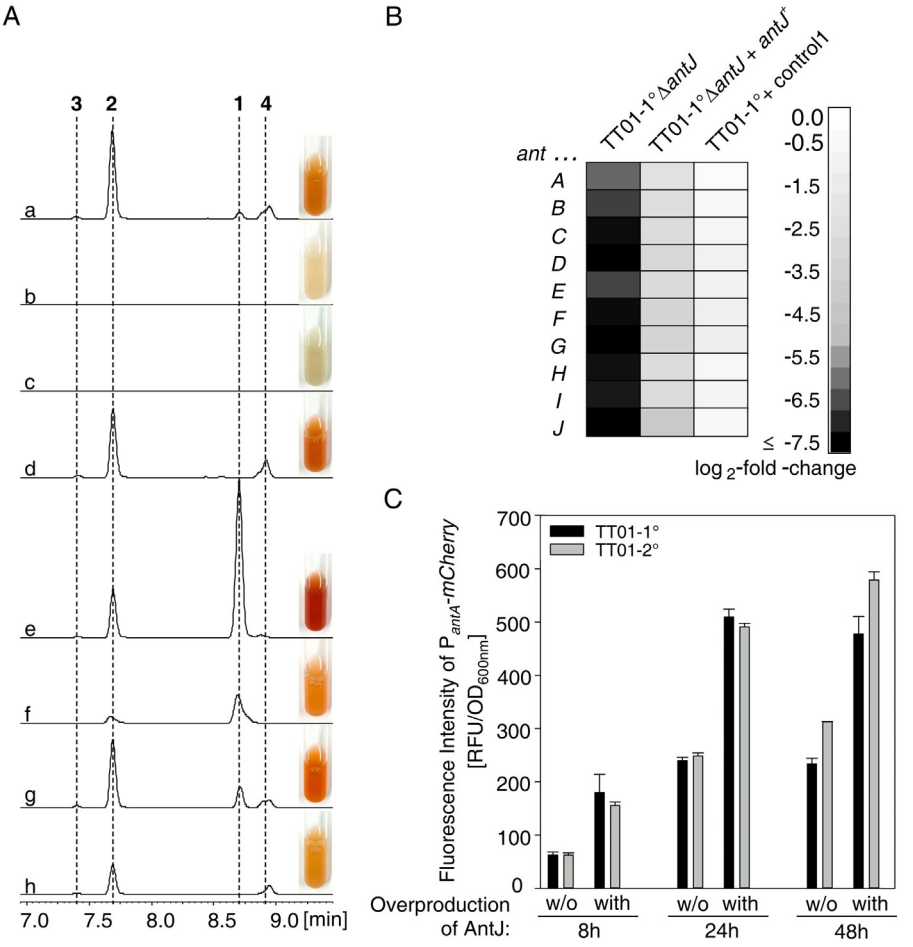

Fig. 2. AntJ activates the promoter of the *antABCDEFGHI* operon and the production of AQs. **A.** Comparison of the AQ production in different *P. luminescens* strains. HPLC-UV analysis (UV-chromatograms at 430 nm) of the ethyl acetate (EE) extracts of a: TT01−1°, b: TT01−2°, c: TT01−1°Δ*antJ*, d: TT01−1° + control 2 (pACYC_tacI/I), e: TT01−1° + $antJ^{++}$ (pAKH05), f: TT01−2° + $antJ^{++}$ (pAKH05), g: TT01−1° + control 1 (pCOLA_tacI/I), h: TT01−1°Δ*antJ* + $antJ^{+}$ (pAKH04), **B.** Heatmap of changes in transcription level of *antA-J* of TT01−1°Δ*antJ* compared to TT01−1° wild type. **C.** Promoter activities of P_{antA} in 1° and 2° cells with and without overproduction of AntJ after 8 h, 24 h and 48 h at the population level. Error bars represent standard deviation of at least three independently performed experiments. RFU, relative fluorescence units.

number plasmid encoding *antJ* (pAKH04) (Fig. 2A, h). AQ production of both wild type 1° cells carrying the empty vector and the complemented 1°Δ*antJ* cells were quantitatively compared by using AQ peak areas (UV-chromatogram at 430 nm) of HPLC-UV analysis normalized to the OD_{600} at the time point of extraction (Fig. S2A) AQ-256 (**1**) was not detectable after 24 h of cultivation in the complemented strain (Fig. 2A, h) since **1** is the starting material for the production of all other AQs and is consumed when other AQs are produced. The amount of AQ-270a and b (**2** and **3**) reached almost 50% of wild type level, and AQ-284 (**4**) production corresponds to 73% of the wild type (Fig. S2A). It is important to

http://dx.doi.org/10.1016/j.heliyon.2016.e00197

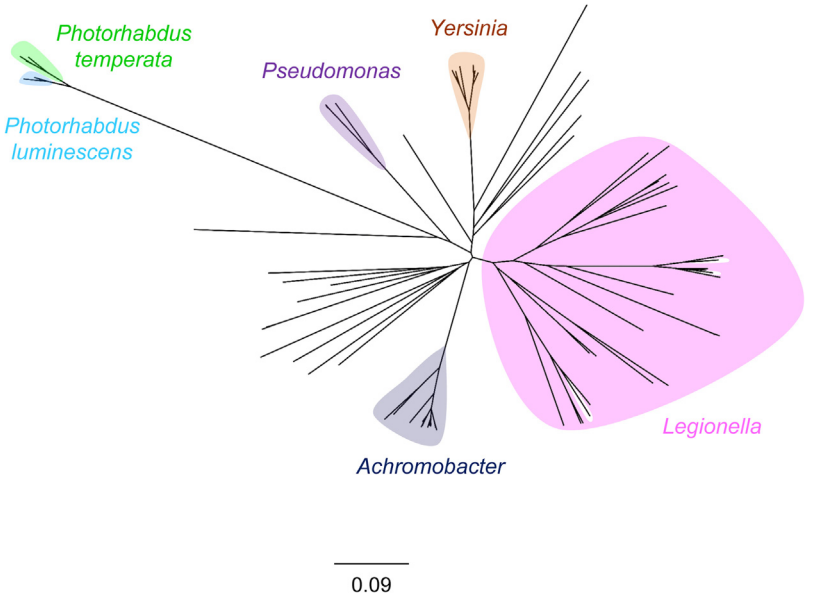

Fig. 3. AntJ is distributed among bacteria that produce secondary metabolites. Neighbour joining dendrogram of AntJ homologues. Sequences are listed in Table S5. Sequences were aligned using clustalW and the tree was generated using the Geneious tree builder incorporated into Geneious (v6.1.8) utilizing the Jukes-Cantor distance model. Scale bar represents amino acid substitutions per amino acid position.

compare the amount of **1**–**4** in total and not separately in order to avoid determining effects caused by small differences in growth of the cultures. Upon overexpression of *antJ* in 1° cells, the production of AQ-256 (**1**) was 46.42 ± 6.04 fold higher compared to wild type, **2** and **3** were present in comparable amounts, whereas **4** was three-fold lower compared to the wild type (Fig. 2A, e and Fig. S2A). Furthermore, a partial pigmentation due to AQ production could be restored in the usually non-pigmented 2° cells by a simple overproduction of AntJ (Fig. 2A, f and Fig. S2B). The production of **1** was 10.00 ± 0.73 fold higher than in the empty vector control of the 1° wild type, whereas **2** and **3** were clearly less produced (0.24 ± 0.01 fold and 0.21 ± 0.05 fold compared to the 1° wild type) and **4** was not detectable at all. Trace amounts of **2** were also detected for 2° cells without overexpression of *antJ* (Fig. S2B).

Moreover, RNA sequencing confirmed a drastic down-regulation of the transcripts *antA-I*, e.g. 195-fold (*antG*) and 72-fold (*antA*), upon deletion of *antJ* in 1° cells (Fig. 2B). Thus, we conclude that AntJ raises the AQ production by activating the transcription of the *antA-I* operon.

However, in the complemented *antJ* deletion strain the mRNA of *antJ* was still 18-fold down-regulated compared to the wild type. In accordance to this finding the transcription level of the *antA-I* genes was also found to be five- to tenfold lower compared to the wild type (Fig. 2B). Other genes, whose transcription was affected

http://dx.doi.org/10.1016/j.heliyon.2016.e00197

to a minor degree via AntJ, included a putative transcriptional regulator (*plu0948*) and a monooxygenase (*plu0947).* Several of the 24 up-regulated mRNAs belong to genes encoding enzymes of the primary metabolism e.g. three genes for fumarate metabolism, seven genes involved in flagella biosynthesis and two genes encoding proteins predicted to play a role in menaquinone biosynthesis of *P. luminescens* (Table S4).

In line with these findings, chemical analysis revealed that the amount of other known secondary metabolites [isopropylstilbene (IPS), GameXPeptides (GXP), photopyrones (PPY) and phurealipids (PL)] [13, 22, 23, 24] is not significantly affected when comparing the wild type with Δ*antJ* and the complemented strain Δ*antJ* + $antJ^{+}$ (Fig. S3A). However, overexpression of *antJ* in the TT01−1° background leads to a reduction of photopyrones and PL A, indicating AntJ acts as some sort of repressor of the genes encoding the ketosynthase PpyS involved in PPY biosynthesis and the methyltransferase PliB responsible for the final PL biosynthesis step. The 2° cells produce less of the other known secondary metabolites compared to the 1° cells and *antJ* overexpression does not enhance the production of these secondary metabolites (Fig. S3B).

Next, we investigated the influence of AntJ on the P_{antA} promoter activity in 1° as well as in 2° cells using a chromosomally integrated P_{antA}-*mCherry* fusion [25]. Unexpectedly, 2° cells exhibited a P_{antA} activity that was comparable to that in 1° cells, when analyzed at the population level. Presence of plasmid-encoded *antJ* increased P_{antA} promoter activity up to twofold both in the 1° and 2° cell population compared to cells carrying the empty vector after 24 h of growth (Fig. 2C).

2.3. AntJ specifically binds within the P_{antA} promoter region

We were further interested in how AntJ positively influences AQ production. As a first step, we quantified the binding of AntJ to the P_{antA} promoter region using surface plasmon resonance (SPR) spectroscopy. For that reason, a double-stranded biotinylated DNA fragment comprising approximately 400 bp upstream of the *antA* gene was immobilized onto a sensor chip that was previously coated with streptavidin. Different concentrations of purified AntJ were then injected over the surface. The sensorgrams revealed a strong interaction of AntJ to the DNA with an overall affinity (K_D) of 100 nM defined by an association rate of $k_a = 1.7 \times 10^5$/M*s and a dissociation rate of $k_d = 0.015$/s (Fig. 4A). However, the sensorgram shapes reveal that the binding mechanism does not reflect a true 1:1 binding event since the curves do not follow a final and linear saturation. This could be due to the fact that the DNA binding mechanism of AntJ is more complex as it has recently been shown for the bacterial response regulator YpdB [26]. Another possible explanation might be that a putative ligand of AntJ is missing, which would further

http://dx.doi.org/10.1016/j.heliyon.2016.e00197

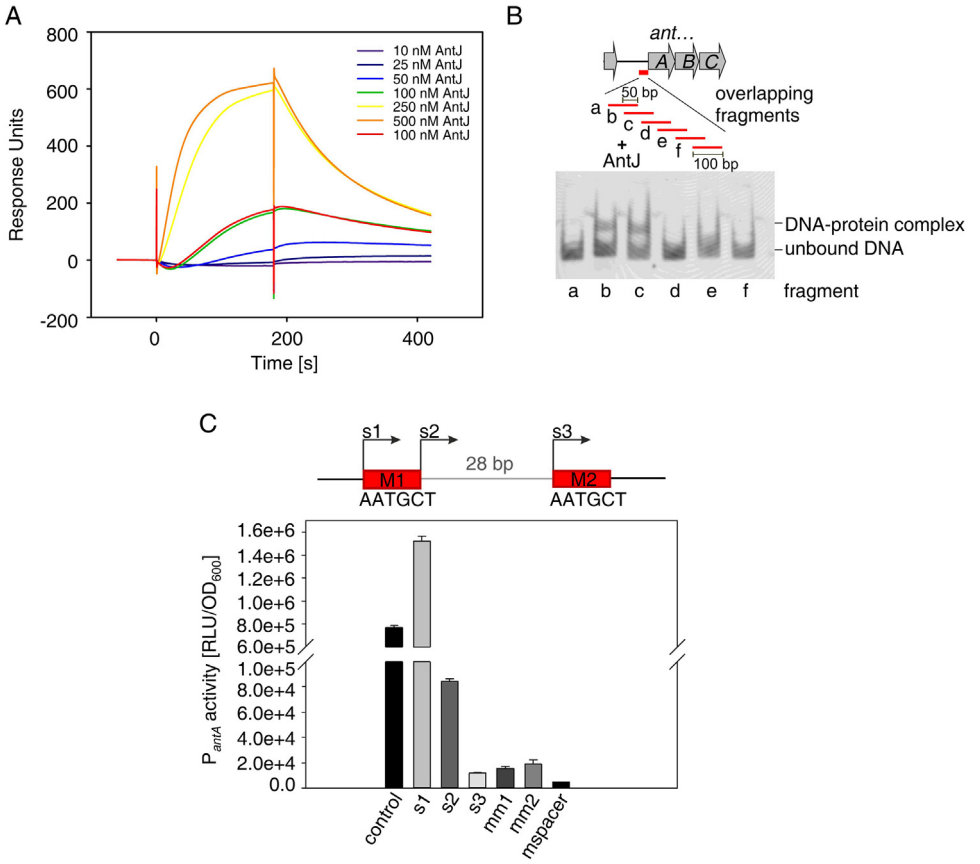

Fig. 4. Characterization of the AntJ DNA-binding site. **A.** Identification of AntJ binding to the *antA* promoter via SPR-spectroscopy. The biotinylated P_{antA} fragment (398 bp) was captured onto a streptavidin-coated sensor chip. Different concentrations of purified His-tagged AntJ (10 nM: purple line; 25 nM: dark blue line; 50 nM: light blue line; 100 nM green and red line; 250 nM: yellow line; 500 nM: orange line) were passed over the chip. AntJ binds to the promoter region of *antA* with an overall affinity (K_D) value of 100 nM. **B.** Determination of a 50 bp long AntJ binding region within the *antA* promoter region via an electrophoretic mobility shift assay (EMSA). Six different 100 bp long fragments (a-f) were chosen comprising the whole promoter region. Each fragment shares a 50 bp overlapping region with its adjacent fragment(s). Fragment b and c contain the AntJ binding region. **C.** Identification of a potential DNA-binding motif of AntJ via reporter gene assays. In the upper panel the potential binding motif of AntJ comprising the two redundant sequences AATGCT (M1 and M2), which are separated via a 28 bp long spacer, is depicted. The lower graph shows a heterologous reporter assay with *E. coli* LMG194 harboring pBAD24-antJ as well as different P_{antA}-*luxCDABE* fusions; control: the complete *antA* promoter, s1-s3: various truncations of the promoter region; mm1: altered potential binding motif 1, mm2: altered potential binding motif 2, mspacer: altered 28 bp long spacer region. The expression of *antJ* was induced via a final concentration of 0.0001% (w/v) arabinose. The graph shows P_{antA} activities in the respective reporter strains after 6 h of growth. Error bars represent SD of at least three independently performed experiments.

stabilize the binding and end in higher association and slower dissociation rates. Next, the binding region was specified to a 50 bp region within P_{antA} via electrophoretic mobility shift assays (EMSA). Six different 100 bp long DNA fragments were used for the binding assays that each shared a 50 bp overlapping

http://dx.doi.org/10.1016/j.heliyon.2016.e00197

region. Only two of these fragments (b and c) were shifted in the presence of AntJ suggesting that the DNA binding region of AntJ is localized within the overlapping 50 bp of DNA (Fig. 4B). This DNA fragment contained two DNA motif repeats "AATGCT" (m1 and m2), which are separated by a 28 bp spacer region. This region was predicted to reflect the specific DNA binding site of AntJ. To verify this hypothesis, we used a heterologous AntJ reporter gene assay. An *E. coli* reporter strain was used that harbors plasmid encoded *antJ* and different P_{antA}-*luxCDABE* promoter fusions. Three different truncations (s1, s2 and s3) of the P_{antA} promoter were tested for P_{antA} promoter activity (Fig. 4C). The s1 truncation starts directly upstream of the first "AATGCT" motif, and exhibited enhanced P_{antA} activity compared to the control P_{antA} fragment revealing that the promoter is intact. However, P_{antA} activity was drastically decreased if the m1 motif was absent (s2) and was further reduced if the spacer region in between m1 and m2 was missing (s3). If the sequence was either modified in motif m1 (mm1) or in motif m2 (mm2) no promoter activity was detectable revealing the specificity of each the m1 and m2 motif within the P_{antA} region for AntJ binding. In contrast to other DNA binding proteins, the spacer region between the m1 and m2 repeat was of functional importance since AntJ was no longer capable of activating the promoter when the sequence of the spacer region was exchanged by a non-sense sequence (mspacer). This reveals that the complete region between m1 and m2 including the spacer is specific and essential for activation of P_{antA} by AntJ.

2.4. P_{antA} promoter activity is heterogeneous at the single-cell level

Since P_{antA} activity was comparable in 1° and 2° cell populations and only 1° cells produce AQs, we investigated P_{antA} activity at the single-cell level. For that purpose, cells harboring a chromosomally integrated P_{antA}-*mCherry* fusion were used, which were generated as described before [25]. Then, the noise value of this reporter strain meaning heterogeneity of P_{antA} activity among single cells was determined. The noise value, also referred to as coefficient of variation (CV), describes the variance of fluorescence between a set of single cells and therefore reflects the overall degree of heterogeneity, whereby a noise value of 1 would reflect a high degree in heterogeneity, and a noise value approaching 0, total homogeneity. For *P. luminescens*, a noise value >0.38 was found to reflect heterogeneity [25]. It could be clearly observed that P_{antA} activity is heterogeneous with a noise value of 0.70 in 1° cells at the single-cell level (Fig. 5). A distinct portion of the cells exhibited a very high promoter activity whereas the other cells showed only a basal, rather weak P_{antA} activity. However, we found a clear *antJ* gene dose effect on the heterogeneous P_{antA} activity. Upon introduction of one additional copy of *antJ* under the control of its native promoter, the heterogeneity was diminished by 39% to a noise value of 0.43 (Fig. 5). The mean fluorescence

 http://dx.doi.org/10.1016/j.heliyon.2016.e00197

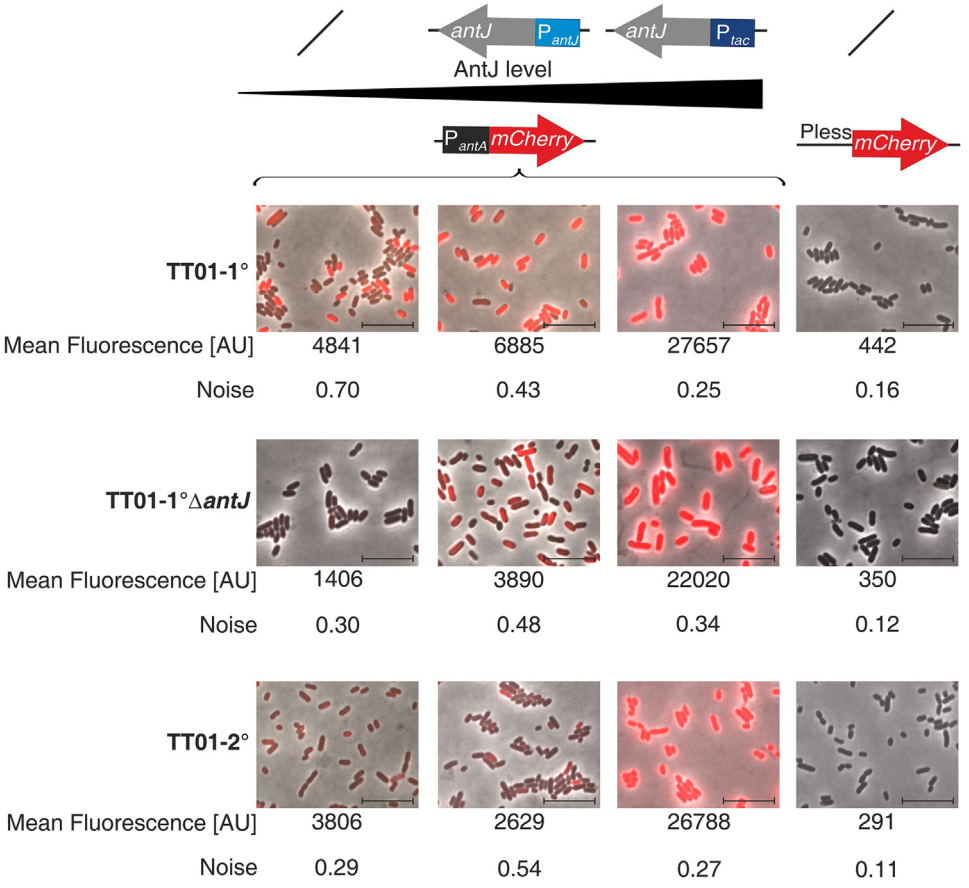

Fig. 5. Heterogeneity of P_{antA} activity at the single-cell level. Single-cell microscopy imaging of *P. luminescens* TT01−1°(A), TT01−1°Δ*antJ* (B) and TT01−2° (C) cells with chromosomally integrated P_{antA}-*mCherry* reporter gene fusion and different levels of AntJ. The pictures at the left panel do not contain additional levels of AntJ and reflect the native conditions. An additional copy of *antJ* was integrated into the genome, which is either under control of the native *antJ* promoter (second from left panel) or the inducible *tac* promoter (second from right panel). A control without a promoter upstream of *mCherry* served as negative control (right panel). The bars in the phase contrast microscopy pictures indicate a scale of 10 µm. The *tac* promoter was induced via the addition of 1 mM IPTG. Additionally, pictures were taken when no IPTG was added (Fig. S5). The pictures depicted are made via overlay of the phase contrast and the fluorophore channel. The fluorescence intensities of 450 single cells were individually measured for each experiment, being analyzed using the software Big Cell Brother [28]. The noise values were calculated as SD/mean from 450 cells after 24 h of growth. Representative images and values from one of three independently performed experiments are shown. For the separate phase contrast and fluorescence pictures see Fig. S8. Box plots that show the distribution of mCherry fluorescence signals and therefore the degree of heterogeneity are presented in Fig. S9. Additionally, AQ production of these reporter strains was measured and compared (Fig. S5 and S6). AU: arbitrary units.

value was 1.4-fold increased, when compared to cells harboring only a single copy of *antJ* (Fig. 5). 1° cells carrying a chromosomal insertion of a P_{tac}-*antJ* gene fusion, exhibited a drastically increased *antJ* expression due to the strong *tac*-promoter and showed a high P_{antA}-activity in the presence and in the absence of the

http://dx.doi.org/10.1016/j.heliyon.2016.e00197

inducer IPTG (Fig. 5, Fig. S4). Upon addition of IPTG, the noise value was decreased to 0.25 indicating total homogeneity, whereas the overall mean fluorescence increased 5.7 fold. As expected, no P_{antA} activity could be observed in 1° cells lacking *antJ* (Fig. 5). However, a heterogeneous P_{antA} activity (noise value of 0.48) could be restored by simple integration of *antJ* at another site of the chromosome. Overproduction of AntJ also mediated a homogeneously distributed P_{antA} activity in the Δ*antJ* background (Fig. 5, Fig. S9). In addition, AQ production correlated with the detected P_{antA} activity in all the reporter strains (Fig. S5 and S6).

Interestingly, a homogeneous P_{antA} activity could be detected in 2° cells (noise value of 0.29). However, the overall mean fluorescence intensity of 1° and 2° cells were comparable (Fig. 5, Fig. S11). By duplicating *antJ* on the chromosome in 2° cells, the heterogeneity of P_{antA} activity increased 1.9 fold, reaching a noise value of 0.54 without detecting any increase in the mean fluorescence values. After integration of an additional copy of *antJ* under control of P_{tac} into the genome of 2° cells, the promoter activity of the anthraquinone operon could be enhanced with a homogeneous pattern and AQ production (only for **2**) was detectable. Contrary to the results presented above (Fig. S2B) no production of **2** could be detected for 2° cells without an additional copy of *antJ* (Fig. S6C).

Relative quantification of the secondary metabolites production showed that all 2° reporter strains produce less of the tested secondary metabolites than the 1° cells (Fig. S7C). Neither one additional copy of *antJ* under the control of its native promoter, nor under the control of P_{tac}, changed the production level of secondary metabolites compared to the respective strain without an additional copy of *antJ* (Fig. S7).

2.5. 1° and 2° cells harbor similar AntJ copy numbers

To test whether heterogeneity of P_{antA} activity is mediated by a different AntJ copy number within individual cells, we generated translational *antJ-mCherry* fusions that are under the control of the native *antJ* promoter. Then, the corresponding P_{antJ}-*antJ-mCherry* elements were integrated into the chromosomes of 1°, 1°Δ*antJ* and 2° cells. However, no significant differences in the fluorescence of the strains could be detected at the single-cell level (Fig. 6A). Additionally, the noise values of 0.19, 0.21 and 0.21 for 1°, 1°Δ*antJ* and 2° cells, respectively, showed a homogeneous distribution of AntJ-mCherry. Furthermore, no autoregulation of AntJ seems to occur since the fluorescence intensity of 1°Δ*antJ* cells did not differ significantly from 1° or 2° wild type cells. We additionally evaluated the transcription levels of *antJ* by quantitative real-time PCR at three different time points of the growth curve (early exponential, late exponential and stationary phase) of 1° and 2° cultures. In relation to the housekeeping gene *recA*, no

 http://dx.doi.org/10.1016/j.heliyon.2016.e00197

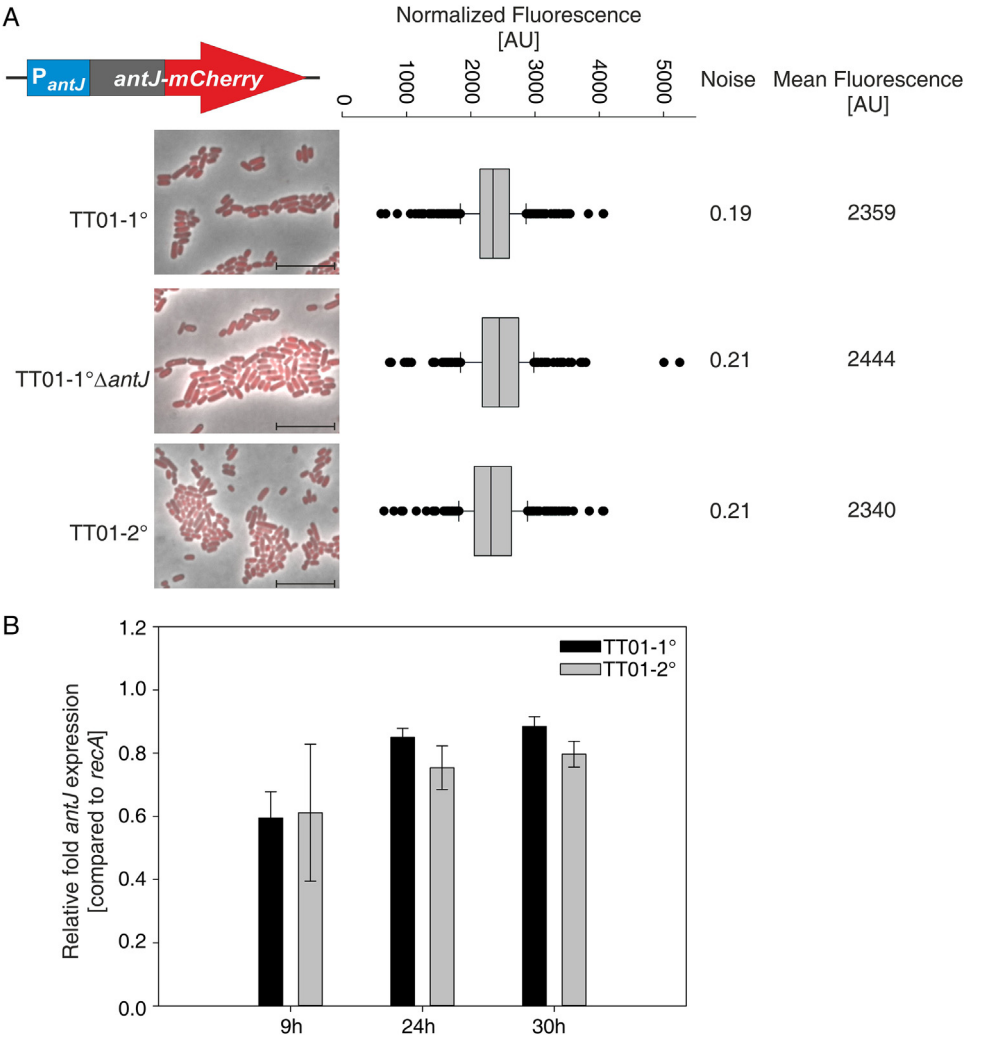

Fig. 6. AntJ levels in *P. luminescens* TT01−1°, TT01−1°Δ*antJ* and TT01–2° cells. **A.** Single-cell microscopy imaging of the three strains with chromosomally integrated P_{antJ}-*antJ-mCherry* constructs. The pictures depicted are made via overlay of the phase contrast and the fluorophore channel. For the separate phase contrast and fluorescence pictures see Fig. S10. The bars in the phase contrast pictures indicate a scale of 10 µm. The fluorescence intensities of 450 single cells were individually measured for each experiment, being analyzed using the software Big Cell Brother [28]. The noise values were calculated as SD/mean from 450 cells. The box plots represent the distribution of mCherry fluorescence signals from 450 cells after 24 h of growth. Representative images and box plots from one of three independently performed experiments are shown. AU: arbitrary units. **B.** The levels of *antJ* transcripts in TT01−1° and TT01–2° cells were determined via qRT-PCR after 9 h (exponential phase), 24 h (late exponential phase) and 30 h (stationary phase) of growth. Changes in transcript levels (expressed relative to *recA*) were calculated using the C_T method [55]. Error bars represent SD of three independently performed experiments.

differences of *antJ*-mRNA could be detected (Fig. 6B). This suggests that heterogeneous P_{antA} activity is not simply mediated by different AntJ copy numbers, but must be directly caused by different AntJ activities in single 1° as

http://dx.doi.org/10.1016/j.heliyon.2016.e00197

well as in all 2° cells. Therefore, AntJ acts as a transcriptional activator of the AQ operon and is, to our knowledge, one of the rare examples causing heterogeneous gene expression by altering its affinity by a yet unknown mechanism rather than its copy number.

3. Discussion

P. luminescens exists in two phenotypically different forms called primary (1°) and secondary (2°). One of the predominant phenotypes specific for 1° cells is pigmentation due to anthraquinone (AQ) production. However, it was unclear how AQ production is regulated. Here we identified a novel type of regulator that we named AntJ, which activates transcription of the *antA-I* operon and therefore AQ production in 1° cells. AntJ is a member of the WYL-domain transcription factors. Within the closest AntJ homologues are transcriptional regulators from different bacteria that are pathogenic to eukaryotes and produce secondary metabolites, i.e., *Legionella, Yersinia* and *Pseudomonas* species. The WYL-domain (generally described as being around 170 aa, Pfam database) in AntJ is predicted to be C-terminally truncated (only 83 aa long). In most bacteria that have close AntJ homologues (i.e. *Pseudomonas, Legionella, Achromobacter, Ochrobactrum* and *Xenorhabdus*), the WYL-domain of the predicted DNA-binding proteins is also C-terminally truncated, indicating that this could be an adaptation for the binding of a similar ligand or binding partner. Interestingly, several species of *Pseudomonas*, *Ochrobactrum* and *Xenorhabdus* have been isolated from (infected) insects whereas the natural reservoirs for *Legionella* are probably amoeba. This is to the best of our knowledge, the first time that a function of a WYL-type regulator has been found that is involved in secondary metabolite production. The distribution of HTH_11/WYL proteins emphasizes the versatility and the importance of this type of regulators. Furthermore, the fact that the AntJ homologue of *P. temperata,* which shows pigmentation, shares a similarity of 93.6% with AntJ of *P. luminescens* whereas no AntJ homologue is found in *P. asymbiotica* implies a highly specific function of AntJ in regulating the pigment production at least in *Photorhabdus* species. The WYL-domain is predicted to be a putative ligand-binding domain whose ligand is still unknown. Until now the WYL-domain has only been found in bacteria [20]. We could show that the AntJ levels in 1° as well as in 2° cells is constant, demonstrating that transcriptional activation of the *antA-I* operon in single 1° cells is not mediated by a simple increase of AntJ. Therefore, a specific activation of AntJ must be mandatory to bind to the P_{antA} promoter and to promote heterogeneity of AQ production. Since the WYL-domain is supposed to act as a ligand-binding domain, activation of AntJ could be due to binding of a specific metabolite or protein in single 1° cells, which does not exist in 2° cells. Homogeneous activation of AQ production due to a simple overexpression of *antJ* in 1° as well as in 2° cells must therefore lead to a ligand-independent activation

 http://dx.doi.org/10.1016/j.heliyon.2016.e00197

caused by the enhanced AntJ copy number in the cells. On the other hand, a putative inhibiting ligand of AntJ cannot be excluded. Whereas one additional chromosomal copy of *antJ* under control of its native promoter did not lead to AQ production in 2° cells, it was indeed sufficient to decrease heterogeneity of P_{antA} activity in 1° cells. Only upon plasmid based overexpression of *antJ* or chromosomal integration of *antJ* with a strong inducible promoter was AQ production detectable in 2° cells. Without additional expression of *antJ* only trace amounts of **2** are detectable in 2° cells. It is obvious that production of AQs in 2° cells can only be achieved upon drastic overproduction of AntJ, so that the influence of a putative inhibiting ligand might be out-competed by high AntJ copy numbers. The presence or absence of a putative ligand must therefore drive activation of AntJ in single cells and mediate heterogeneity of P_{antA} activation as a noise generator. A similar system has already been described for Spo0A in *Bacillus subtilis*. Spo0A is a master regulator for spore formation and is only active when phosphorylated. The heterogeneous activation of Spo0A is achieved by a limiting phosphate flux. Only upon a certain threshold of phosphorylated Spo0A within the cell, sporulation is induced [27]. Another example for regulation of phenotypic heterogeneity by a noise of phosphorylation is bioluminescence in *Vibrio harveyi* [28]. The ratios between kinase and phosphatase activities of the three sensor kinases and hence the phosphorylation state of the response regulator LuxO is not only important for the signal output, but also for the noise of the system and therefore of light production in single cells. However, it is unlikely that AntJ activity is also driven by a heterogeneous post-translational modification like Spo0A or LuxO. Moreover, several examples for heterogeneity in quorum sensing exist, where the respective LuxR-type receptor binds the auto-inducer signal(s) and therefore regulates heterogeneous gene expression (see [4] for review). Therefore, we would suppose a similar mechanism for AntJ and the putative yet unknown ligand to mediate heterogeneous AQ gene expression.

A global regulator that mediates phenotypic heterogeneity in *Photorhabdus* is HexA, which was identified as global transcriptional regulator and repressor of secondary metabolism [29, 30]. The influence of HexA on symbiosis was valued when exploring that 2° cells of *P. temperata* restore the ability to support nematode development upon inactivation of *hexA*. Therefore, HexA seems to be responsible for the lack of symbiosis factors in 2° cells [29]. However, there are no differences in heterogeneity of P_{antA} activity in 1°Δ*hexA* cells detectable (our own observation), so that variable HexA copy numbers in single 1° cells as well as enhanced HexA levels in 2° cells do obviously not influence AntJ heterogeneity of AQ production.

The absence of the global regulator HdfR (Plu4688) harms symbiosis due to the incapability of *P. luminescens* cells to realize the transmission of the symbiont [31]. Interestingly, deletion of *hdfR* altered the transcription level of 124 genes

http://dx.doi.org/10.1016/j.heliyon.2016.e00197

including the *antA-I* operon, which was down-regulated in 1°Δ*hdfR* cells. However, we could not co-elute HdfR with the P_{antA} promoter, suggesting that HdfR indirectly influences *antA-I* expression, possibly by regulation of the putative ligand that interacts with AntJ. Other regulators binding to the P_{antA} region were the LysR-type regulator Plu2548 and the LuxR-like protein Plu0919. However, a deletion of the respective genes did not show any alterations in the pigmentation, so that these regulators are not supposed to be responsible for heterogeneous P_{antA} activation.

In other AQ producing organisms, little is known about the regulation of AQ synthesis. Cultures of *Morinda citrifolia* plant cells are capable of using chorismate as starting material for the production of AQs. However, no specific regulator has yet been identified. It is known that in *M. citrifolia* AQ production is dependent on the activity of the enzyme isochorismate synthase, which leads chorismate to AQ

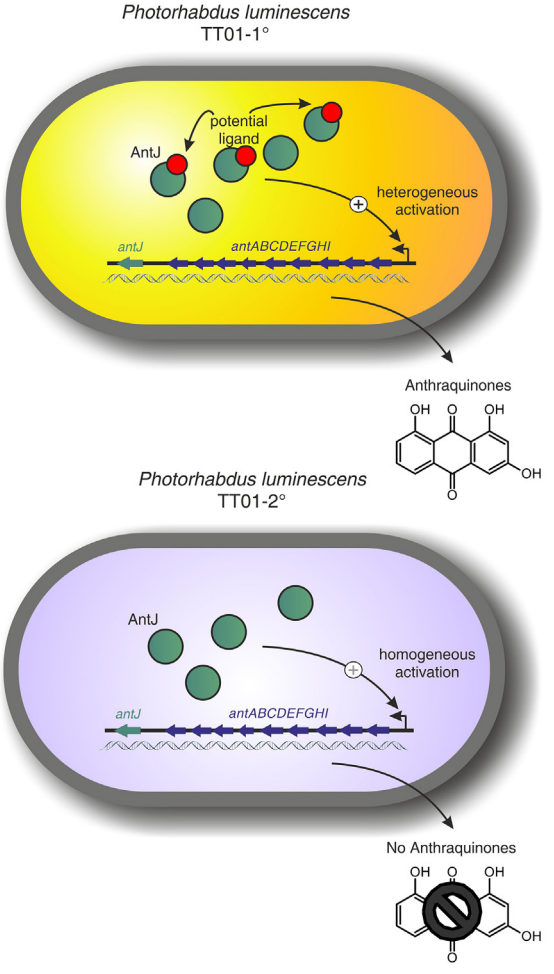

Fig. 7. Model of the regulation of AQ production in *P. luminescens* 1° and 2° cells by AntJ. 1° cells are depicted in yellow, 2° cells in cyan. The putative activating ligand of AntJ is shown in red.

http://dx.doi.org/10.1016/j.heliyon.2016.e00197

synthesis [32]. Comparable to that a correlation between a higher concentration of the starting material malonyl-CoA within the cell and enhanced production of AQs has also been proposed in *P. luminescens* [11]. Similar as in *P. luminescens* it was shown in *Aspergillus fumigatus* that a global regulator of secondary metabolism, LaeA, regulates the biosynthetic genes for AQ production, but the detailed regulatory mechanism is not understood [33]. However, heterogeneous AQ production has neither been described in *Aspergillus fumigatus* nor in *Morinda citrifolia.*

It has been demonstrated before that both stochasticity, inherent in the biochemical process of gene expression, and fluctuations in other cellular components can contribute to overall variation of gene expression in single cells, that were referred to as intrinsic and extrinsic noise [34]. Since AntJ copy number is constant in 1° as well as in 2° cells it can be concluded that noise of AntJ activity is mainly caused by extrinsic noise of a specific ligand. A basic principle of phenotypic heterogeneity has been described due to noise based on molecules that exist in low copy numbers within a cell [35]. Consequently, the cellular state corresponding to the molecular composition of a cell and its gene expression phenotype varies over time and between individual cells. Specific sources of this variation can include stochastic gene expression [36] and stochastic partitioning of molecules at cell division [37]. Another molecular mechanism that can result in phenotypic heterogeneity independent of a specific ligand is the epigenetic modification of the DNA caused by differences in DNA modification like methylation. Those epigenetic modifications are an important source of phenotypic heterogeneity in eukaryotic microorganisms [38, 39]. It could be possible that 1° and 2° cells differ in their overall modification of the DNA, but however this has not been described yet. Moreover, such a phenomenon could indeed explain the absence of AQ biosynthesis in 2° cells, but not the heterogeneity of P_{antA} activation in single 1° cells. The heterogeneity in AQ production of 1° cells is a typical example of division of labor [35] since production of AQ and secondary metabolites in general can require a large fraction of the celĺs genomic and metabolic resources [40] and is therefore cost-intensive. Since the AQs are secreted it is sufficient that only a part of the population invests the energetic costs for AQ biosynthesis, whereas the whole population can benefit from it.

In summary, we propose that the presence of a putative ligand of AntJ at a certain concentration promotes noise and therefore heterogeneity of AQ production in 1° cells, whereas the predominant presence or the total absence of this ligand is the reason for the lack of AQ production in 2° cells. However, the mechanism of a ligand activating AntJ, which is from our point of view more likely, is illustrated in Fig. 7. Overall, AntJ is a novel type of transcriptional activator and one of the rare examples yet that mediates heterogeneous gene expression by altering its activity

http://dx.doi.org/10.1016/j.heliyon.2016.e00197

rather than its copy number. The identification of the putative ligand that might bind to AntJ remains to be elusive.

4. Material and methods

4.1. Strains, plasmids and oligonucleotides

All strains used in this study are listed in Table S1, all plasmids in Table S2 and oligonucleotides in Table S3.

4.2. Molecular biological methods

DNA manipulation was performed following standard procedures [41]. For isolation of genomic DNA from *P. luminescens* TT01 Gentra Puregene Yeast/Bact Kit (Qiagen, Hilden) or Ultra-Clean Microbial DNA Isolation Kit (Mo Bio Laboratories Inc., Carlsbad) were used. Polymerase chain reaction (PCR) was done with Phire Hot Start II DNA polymerase (Thermo Scientific, Darmstadt), OneTaq polymerase (New England Biolabs, Frankfurt) or Q5 polymerase (New England Biolabs, Frankfurt) according to the manufacturer's instructions. Oligonucleotides were purchased from Eurofins Genomics. The MinElute PCR Purification Kit (Qiagen, Hilden) or HiYield® PCR DNA Fragment Extraction Kit (Südlabor, Gauting) was used for DNA purification from agarose gels. Plasmid isolation was performed with the Invisorb® Spin Plasmid Mini Two Kit (Stratec, Birkenfeld) or HiYield® Plasmid Mini Kit (Südlabor, Gauting). DNA restrictions were performed following the manufacturer's protocol using endonucleases from Thermo Scientific (Darmstadt) or New England Biolabs (Frankfurt).

4.3. Bacterial strains and culture conditions

P. luminescens and *E. coli* were aerobically grown in LB medium [41] at 30 °C (*P. luminescens*) and 37 °C (*E. coli*). For agar plates 1.5% (w/v) agar was added to the media. If necessary, media were supplemented with chloramphenicol (20 μg/ml), kanamycin (50 μg/ml), gentamycin (15 μg/ml), ampicillin (100 μg/ml) and/or rifampicin (50 μg/ml). The plasmid-based *antJ* overexpression in the *P. luminescens* TT01−1° + $antJ^{++}$ (pAKH05) and TT01−2° + $antJ^{++}$ (pAKH05) was induced with 0.1 mM IPTG. Expression of chromosomal P_{tac}-*antJ* was induced upon addition of 1 mM IPTG. In order to avoid overexpression of *antJ* in *P. luminescens* TT01−1°Δ*antJ* + $antJ^{+}$ (pAKH04), P_{tac} was not induced and *antJ* expression was achieved as result of the basal promoter activity. For growth of *E. coli* ST18 the medium was supplemented with 5-aminolevulinic acid (50 μg/ml) [42]. Pre-cultures were grown overnight and the following day appropriate volumes of the pre-cultures were used for inoculation of the main cultures to an OD_{600} = 0.05 (fluorescence microscopy) or OD_{600} = 0.1 (chemical analyses). All strains are listed in Table S2.

http://dx.doi.org/10.1016/j.heliyon.2016.e00197

4.4. Generation of the plasmids

To complement *antJ* in the TT01−1°Δ*antJ* deletion strain and for overexpression of *antJ* in the wild type, the entire coding sequence of *antJ* was amplified from genomic DNA of *P. luminescens* using primers AKHp14 and AKHp15. Using these primers on both ends of the insert a 24 bp overhang homologous region to pCOLA_tacI/I or pACYC_tacI/I respectively, was added to enable Gibson assembly. The backbones of pCOLA_tacI/I and pACYC_tacI/I were amplified by PCR using primers AKHp12 and AKHp13. Assembled products (pAKH04 and pAKH05) were used to transform *E. coli* DH10B. Plasmids were isolated and transferred into strains TT01−1°Δ*antJ* and TT01−1° or TT01−2°, respectively.

For the purification of AntJ used for SPR spectroscopy, the plasmid pBAD24-antJ-His was generated via amplification of *antJ* (728 bp) using primers antJ-NheI_fwd and antJ-NdeI-ostop_rev. The insert and the vector were cut with restriction enzymes NheI and NdeI. The correct insertion was verified via PCR using primers pBAD24-seq_fwd and pBAD24-seq_rev.

For the purification of AntJ used in EMSA assays the plasmid pCATI4_antJ was constructed. For that purpose *antJ* was amplified with the primers AKHp44/45 and to both ends of the insert an overhang homologous to pCATI4 was attached for Gibson assembly. The vector pCATI4 was amplified by PCR using primers AKHp42/43. *E. coli* DH10B was transformed with the assembled vector. The vector insert was verified via sequencing.

For reporter assays in *E. coli* LMG194, the plasmid pBAD24-antJ was generated via amplification of *antJ* with the primers antJ-NheI_fwd and antJ-NdeI_rev (731 bp) and subsequent cleavage of the insert and the vector via NheI and NdeI. The different constructs of the *antA* promoter region were cloned into the plasmid pBBR1-mcs5-tt-lux. The complete promoter was amplified with the primers PantA-XbaI_fwd and PantA-XmaI_rev (389 bp). For generation of the *antA* promoter derivatives s1 (241 bp), s2 (239 bp) and s3 (203 bp), the primers PantA-s1-XbaI_fwd, PantA-s2-XbaI_fwd and PantA-s3-XbaI_fwd were used and each primer was combined with PantA-XmaI_rev for PCR. The construct mm1 (398 bp PCR) was generated via an overlap-PCR (PantA-XbaI_fwd, PantA-XmAI_rev) of the products that had been amplified with the primers pairs PantA-XbaI_fwd, PantA-mm1-ol_rev and PantA-mm1-ol_fwd and PantA-XmaI_rev. The construct mm2 (398 bp) was made via an overlap-PCR (PantA-XbaI_fwd, PantA-XmAI_rev) of the products that had been amplified with the primer pairs PantA-XbaI_fwd, PantA-mm2_rev and PantA-mm2_fwd, PantA-XmaI_rev. For construction of the mspacer (398 bp) two PCRs with the primer pairs PantA-XbaI_fwd, PantA-spacer-ol_rev and PantA-spacer-ol_fwd, PantA-XbaI_rev and a subsequent overlap-PCR as described above were performed. All of the PCR products were cut with restriction enzymes XbaI and XmaI and subsequently

http://dx.doi.org/10.1016/j.heliyon.2016.e00197

ligated with equally treated vector pBBR1-mcs5-tt-lux. Correct insertions were verified via control-PCR using the primers check-pBBR_fwd and check-pBBR_rev.

A PCR was performed to amplify *eyfp* with a size of 757 bp by using the primers eyfp-mcs_fwd and eyfp-EcoRI_rev and the plasmid pEYFP as a template. The PCR product and the vector pPINT-mCherry [25] were cut with the enzymes ApaI and EcoRI and the resulting plasmid was called pPEINT-mCherry. The control-PCR was performed using the primers check-mcherry-ins_rev and check-eyfp2_rev with a resulting PCR size of 1106 bp.

In order to generate the *eyfp* fusions three different constructs were inserted into pPEINT-P_{less}-mCherry-P_{less}-eyfp. P_{antJ} (519 bp) was generated via PCR using primers PantJ-NheI_fwd and PantJ-Not_rev and for generation of P_{antJ}-*antJ* (1220 bp) primers PantJ-NheI_fwd and antJ-ostop-NcoI_rev were used. For generation of both PCR products chromosomal DNA of *P. luminescens* was used as template.

P_{tac}-*antJ* was amplified via Ptac-antJ-NheI_fwd and antJ-ostop-NcoI_rev, containing the *lacI* repressor gene and *antJ* under the control of the *tac*-promoter. The plasmid pAKH05 was used as template and the product size was 2110 bp.

A PCR was performed to generate P_{antA}-*mCherry* fusions for all three plasmids. P_{antA} was amplified by a PCR with the primers PantA-NheI_fwd and PantA-NheI_rev and the PCR product was cut with NheI. The proper insertion within the correct direction was verified via DNA sequencing. The resulting plasmids were called pPEINT-P_{antA}-mCherry-P_{antJ}-eyfp, pPEINT-P_{antA}-mCherry-P_{antJ}-*antJ*-eyfp and pPEINT-P_{antA}-mCherry-P_{tac}-*antJ*-eyfp. A control PCR with the primers check-mcherry-ins_rev and check-eyfp _rev was performed.

For generation of the plasmids pPINT-P_{antJ}-mCherry and pPINT-P_{antJ}-*antJ*-mCherry the following procedures were performed. P_{antJ} was amplified via the primers PantJ-NheI_fwd and PantJ-BamHI_rev resulting in a 516 bp product and the 1215 bp long P_{antJ}-*antJ* product was generated with the primers PantJ-NheI_fwd and antJ-ostop-BamHI_rev. For both PCR products, chromosomal DNA of *P. luminescens* was used as template. In order to insert P_{antJ} and P_{antJ}-*antJ* upstream of *mCherry,* the vector pPINT-mCherry as well as the inserts were cut with NheI and BamHI. The resulting plasmids were called pPINT-P_{antJ}-*mCherry* and pPINT-P_{antJ}-*antJ-mCherry*. The correct insertions were verified by a PCR with the primers check-mcherry-ins_rev and check-eyfp-ins_rev. Furthermore, all generated plasmids were sequenced (Genomics core facility, LMU Biozentrum) to verify correctness.

http://dx.doi.org/10.1016/j.heliyon.2016.e00197

4.5. Competent cells and transformation

E. coli cells were made chemically competent and transformed as described elsewhere [43].

4.6. Generation of knockout mutants

The gene encoding AntJ (*plu4185*) was deleted using pCKcipB [24], which is a derivative of pDS132 [44]. For the in frame deletion of *antJ* an upstream (926 bp) and a downstream fragment (788 bp) of *antJ* were amplified by PCR using primers AKHp06–AKHp09 introducing a PstI and a BamHI restriction site to the 5′end of the upstream fragment and the 3′end of the downstream fragment, respectively. Splice overlap extension was used to fuse the two PCR products, which were subcloned into pJET1.2, digested using PstI and BamHI restriction sites and cloned into pCKcipB via the PstI and BglII restriction sites. The resulting plasmid pAKH01 was transferred by electroporation into *E. coli* S17-1 λ*pir*. Transformants were confirmed via plasmid extraction and restriction analysis before using for conjugation with *P. luminescens* TT01. Conjugation and plasmid excision via a second homologous recombination were performed as described before [14]. In order to confirm the 702 bp markerless deletion of *antJ* primers AKHp10 and AKHp11 were used. For the deletion of the genes *plu0918-0925* and *plu2548 a* similar strategy was applied. Upstream and downstream regions were amplified using primers AKHp16-19 and AKHp22-25, respectively. In this way both upstream/downstream fragments were each extended with a 20 bp/25 bp stretch homologous to the vector and a 12–13 bp overlap homologous to the other fragment. Related up- and downstream fragments were cloned into pCKcipB, linearized with PstI and BglII using Gibson Cloning (Gibson Assembly Cloning Kit, New England Biolabs GmbH). Deletion of 7498 bp or 887 bp were confirmed by PCR using primers AKHp20-21 or AKHp26-27.

4.7. Reporter gene assays

For promoter activity assays in *E. coli* LMG194, cells were inoculated at an OD_{600} of 0.05 and aerobically grown at 37 °C in microtiter plates within a Tecan Infinite F500 system (Tecan). OD_{600} and luminescence were measured every 10 minutes for 8 h. Arabinose was added at a final concentration of 0.0001% (w/v) after the cells reached an OD_{600} of 0.2. Data are reported as relative light units (RLU) in counts per second per milliliter per OD_{600}.

For reporter activity assays with *P. luminescens*, the OD_{600}, which initially was adjusted to 0.05, the cells were aerobically grown at 30 °C in microtiter plates with a Tecan Infinite F500 system (Tecan). The OD and fluorescence intensity of mCherry (560 nm excitation, 612 nm emission, 20 nm bandwidth) were measured after 8, 24 and 28 h of incubation. Data are reported as relative fluorescence units

http://dx.doi.org/10.1016/j.heliyon.2016.e00197

(RFU). Raw fluorescence data were normalized with the optical density (OD_{600}) of the respective culture.

4.8. DNA-protein pull down assay

For the DNA-protein pull down assay the upstream region of *antA* (986 bp) was amplified by PCR into three overlapping fragments using the primers AKHp01-05. All forward primers were biotinylated. The PCR products were excised after gel electrophoretic separation. Following agarose digest and isopropanol/glycogen precipitation, the DNA was re-dissolved in distilled water. Dynabeads® M-280 Streptavidin were used according to the manufactureŕs protocol (Invitrogen, Life Technologies). 100 µl of the Dynabeads® were loaded with 3 µg of the purified DNA fragment. *P. luminescens* was grown to an OD_{600} of 5.4 and harvested cells were stored at −20 °C. A cell pellet from 100 ml culture was resuspended in 5 ml lysis buffer [50 mM tris(hydroxymethyl)aminomethane Tris/HCl, pH 7.4, 5 mM ethylenediaminetetraacetic acid (EDTA) disodium salt, 100 mM NaCl, 1 mM dithiothreitol (DTT), 0.05% (v/v) Triton X–100, 1:200 protease inhibitor mix (Protease Inhibitor Cocktail SetIII, EDTA free, Calbiochem®) a spatula tip lysozyme]. For completion of cell lysis as well as destruction of cellular DNA the cell suspension was sonicated. Unsolvable cell fragments were removed by centrifugation. 3 µg promoter fragment (immobilized on the Dynabeads®) were incubated together with 10 µg salmon sperm DNA with 1.4 ml cell lysate. After 15 min of incubation, washing steps (15 min) with increasing salt concentration were performed [125/150/175/200 mM NaCl in 50 mM Tris/HCl, pH 7.4, 1 mM DTT, 0.05% (v/v) Triton X–100, 1:1000 protease inhibitor mix]. Final elution of the proteins was realized by incubation with 500 mM NaCl in 50 mM Tris/HCl, pH 7.4 for 30 min. The proteins in the cell lysate, in the washing steps (W1-W4) and the elution fraction were harvested using chloroform/methanol precipitation [45].

4.9. Peptide mass fingerprint

The dried protein pellets were solved in protein loading dye [20 mM Tris HCl, 4% glycerin, 2% (w/v) SDS, 0.3 M β-mercaptoethanol, 0.04% (w/v) bromophenol blue, pH 6.8] and proteins were size depended separated using SDS-PAGE. Bands of interest were excised from Coomassie Blue G-250 stained gels and in-gel digested with slight modifications as described earlier [46]. Reduction and alkylation were performed as described in [46] (step 4.A). Prior to overnight digestion at 37 °C in 60 µl digestion buffer [10 ng μl^{-1} trypsin, 10% (v/v) ACN, 10 mM NH_4HCO_3] the gel slice was washed three times with 50% 100 mM NH_4HCO_3/50% acetonitril (ACN) for 10 min, and then with ACN for 10 min. Peptide extraction was performed for 30 min at 37 °C with 30% ACN/0.1% trifluoroacetic acid (TFA) followed by a second extraction with 50% ACN/0.1% TFA. Both extracts were

http://dx.doi.org/10.1016/j.heliyon.2016.e00197

mixed and dried under reduced pressure. Afterwards the peptides were dissolved in 20 µl 30% ACN/0.1% TFA and measured with MALDI MS.

4.10. MALDI MS analysis and Mascot database search

MALDI MS analysis and sample preparation was described earlier [47]. The samples were 1:1 mixed with the matrix [20 mM 4-Chloro-α-cyanocinnamic acid (ClCCA) solved in 70% (v/v) ACN] on a MALDI-Target and air-dried. Spectra were analyzed with the Qual Browser (Version 2.0.7; Thermo Fisher Scientific, Inc., Waltham) and used for a database search on the mascot server (matrixscience.com) applying the following parameters: peptide mass fingerprint database: NCBInr; enzyme: trypsin (3 missed cleavages allowed); fixed modification: carbamidomethyl (C); variable modification: oxidation (M); peptide tolerance: 5 ppm; mass values: MH+, monoisotopic.

4.11. Integration of reporter genes into the genome of *P. luminescens*

In order to integrate P_{antA}-*mCherry* as well as the P_{antJ}, P_{antJ}-*antJ* and P_{tac}-*antJ* constructs into the genome of *P. luminescens*, the donor strain *E. coli* ST18 [42], which requires the addition of 5-aminolevulinic acid for growth, was first transformed with the respective plasmids. The conjugative plasmid transfer was subsequently performed by the filter mating method [42]. For that reason, the donor as well as the recipient strain was cultivated up to an OD_{600} of 0.8–1. The donor strain was washed in LB medium for 3 times and then mixed with the recipient strain in a ratio of 1:5 in a final volume of 1/10 of the donor‘s initial volume. A nitrocellulose filter was set onto an LB agar plate and the mixed cells were then dropped onto the filter without dispersion. After the incubation at 30 °C over-night, the cells were re-suspended in 500 µl LB and spread onto LB agar plates containing kanamycin and incubated for up to two days at 30 °C. The genomic DNA of single colonies were isolated and used as a template to check for chromosomal integration of the plasmid via PCR (primers: check-rpmE_fwd, oriT_fwd, gmR-pNPTS_fwd, check-mcherry-ins_rev, check-glmS_rev). As all the strains yielded additionally P_{antJ}-*eYFP*, P_{antJ}-*antJ-eYFP* and P_{tac}-*antJ-eYFP* (no induction) that had no fluorescence effect, the reporter strains are just referred to as P_{antJ}, P_{antJ}-*antJ* and P_{tac}-*antJ*.

4.12. Transcription analyses using quantitative real-time PCR (qPCR)

P. luminescens 1° and 2° cells were cultivated as described above. Samples were taken at 9 h, 24 h and 30 h of growth before the total RNA was isolated using the Quick RNA Mini prep kit (Zymo Research, Freiburg im Breisgau). The RNA was

http://dx.doi.org/10.1016/j.heliyon.2016.e00197

then re-transcribed to cDNA via the random-primed first-strand cDNA synthesis kit (Thermo Scientific, Dreieich). Quantitative real-time PCR (iQ5 real-time PCR detection system, BioRad, München) was performed using the synthesized cDNA, a SYBR green detection system (BioRad, München) and specific internal primers for *antJ* and *recA*. Samples from three independently performed experiments were used and the C^t value (cycle threshold) was determined after 40 cycles using the iQ software (BioRad, München). Values were normalized with reference to *recA* and relative changes in transcript levels were calculated using the comparative $\Delta\Delta C^t$ method [48].

4.13. RNA extraction and sequencing

For RNA sequencing, the respective *P. luminescens* strains were inoculated in LB broth with an OD_{600} of 0.3 with pre-cultures grown in the same medium. After 8–10 h of aerobic cultivation at 30 °C cells were harvested (OD_{600} = 5) and for extraction of total RNA, cells from 1 ml culture were re-suspended in 800 µl AE-buffer [20 mM NaOAc, 1 mM EDTA (pH 5.2) made in nuclease free water], mixed with 500 µl acidified phenol:chloroform and after transfer to a homogenization tube (lysing matrix B: 0.1 mm silica spheres, MP Biomedicals Germany GmbH) disrupted using a cell homogenizer (FastPrep-24^R 5G, MP Biomedicals Germany GmbH) with two cycles of 30 s at 6 m s^{-1}. After phase separation the aqueous phase was extracted two times with 500 µl of chloroform. Finally, the RNA was precipitated by adding 600 µl isopropanol and 120 µl 3 M sodium acetate at −20 °C overnight. The RNA was pelleted and washed twice with ice cold 70% (v/v) ethanol, dried on ice and re-suspended in 35 µl nuclease free water. Then DNase treatment (TURBO DNA-free^{TM} Kit, Life Technologies) was performed following the manufacturer's instructions. Eurofins Genomics GmbH (Ebersberg, Germany) performed RNA quality control and rRNA depletion immediately before sequencing the RNA samples. Data is available at the European Nucleotide Archive (ENA) using accession number (ERP018162). During sequencing, directionality of the reads was maintained and all sequencing data was mapped to the *P. luminescens* TT01 genome [49] using the bowtie function as a part of Nesoni (v0.128). The count function from Nesoni (v0.128) was subsequently used to count before analysing with Limma/Voom, which is part of Degust (v0.19 available at http://www.vicbioinformatics.com/degust/). A false discovery rate (FDR) of <0.01 was used and only sequences which were at least 1.5-fold up-/down-regulated compared to the WT were considered significant. Transcripts with more than 2.5-fold altered expression level in the empty vector control (TT01−1° + control1) compared to the WT were excluded (Table S4).

http://dx.doi.org/10.1016/j.heliyon.2016.e00197

4.14. Analytical scale culture extraction and HPLC-UV/MS analysis

P. luminescens strains were inoculated in LB media in 100 ml Erlenmeyer flasks with an overnight culture to an OD_{600} of 0.1 and aerobically grown for 24 h at 30 °C. For ethyl acetate (EE) extractions 2 ml samples of the cultures were extracted for 1 h at RT with 2 ml EE + 0.1% FA. 1 ml of the organic supernatant was dried under nitrogen flow. The extracts were re-dissolved in 250 µl methanol and measured by HPLC-UV/MS. HPLC-UV/MS analysis was done as explained before [50]. We used an ACN/0.1% FA in H_2O/0.1% FA gradient from 5 to 95% in 12 min at a flow rate of 0.6 ml/min at 30 °C. Chromatograms were analyzed using Bruker Compass DataAnalysis 4.2. For AQ quantification peak areas of the HPLC-UV analysis (UV-chromatograms at 430 nm) were used. For SM quantification, peak areas of the HPLC-MS chromatogram were determined using Bruker Compass TargetAnalysis Version 1.3. The respective peak areas were normalized against the cell density (OD_{600}) when cultures were harvested.

4.15. Fluorescence microscopy and single-cell analysis

The *P. luminescens* fluorescence reporter strains were investigated using a fluorescence microscope (Leica, Bensheim, Germany). An excitation wavelength of 546 nm and a 605 nm emission filter with a 75 nm bandwidth was used to measure mCherry. The cultures were inoculated at an OD_{600} of 0.05 with the appropriate volume of the respective over-night cultures, and were then grown at 30 °C for 24 h in the presence of appropriate antibiotics. An agarose pad [0.5% (w/v) agarose in PBS buffer, pH 7.4] was prepared onto a microscope slide, 7 µl of the grown cultures were dropped onto the slide and covered with a coverslip. Three independent biological experiments were performed. For each experiment, the fluorescence intensities of 450 cells were measured using the single-cell analysis tool Big Cell Brother [28].

4.16. Purification of AntJ

For purification of AntJ for SPR analysis, *E. coli* BL21 was transformed with plasmid pBAD24-antJ-His. The cells were cultivated up to an OD_{600} of 0.5 and then gene expression was induced by the addition of 0.5 mM IPTG. After 3–4 h of aerobic cultivation at 30 °C the cells were harvested by centrifugation (6500 rpm, 15 min, 4 °C). After harvesting the cells were disrupted via using a Cell disruptor (Constant Cell Disruption Systems, Northants, UK) at 1.35 kbar and 4 °C in lysis buffer [50 mM Tris/HCl pH 7.5, 10% (v/v) glycerol, 10 mM $MgCl_2$, 1 mM dithiotreitol, 0.5 mM phenylmethylsulfonylfluoride, and 0.03 mg/ml (w/v) DNase]. After removal of intact cells and cell debris by centrifugation (9.000 × g, 10 min), the cytosol was frozen at −80 °C. Purification was carried out as described before

http://dx.doi.org/10.1016/j.heliyon.2016.e00197

[51]. The equilibration and washing steps were performed in buffer E [50 mM Tris/HCl, pH 7.5, 10% (v/v) glycerol, 200 mM NaCl, 2 mM β-mercaptoethanol, 10 mM imidazole], and 250 mM imidazole was added for the elution of the protein from the column.

For purification of AntJ for EMSA experiments, *E. coli* BL21 Star (DE3) was transformed with plasmid pCATI4_antJ. Cells were aerobically grown at 30 °C in autoinduction medium [LB medium supplemented with 3.3 g/l $(NH_4)_2SO_4$, 6.8 g/l KH_2PO_4, 7.1 g/l Na_2HPO_4, 5 g/l glycerol, 0.5 g/l glucose and 2.0 g/l α-lactose] [52]. After 24 h cells were harvested (30.000 x g, 15 min, 4 °C) and pellets were stored at −20 °C. Cell lysis and protein purification were performed as described before [53]. Apart from this all buffers were adjusted to pH 7 and contained additionally 10% (v/v) glycerol and 0.1% Triton X–100 in order to improve solubility of AntJ. Purified AntJ was immediately used for EMSA experiments.

4.17. Electrophoretic mobility shift assay (EMSA)

Labeling of DNA regions for EMSA experiments was performed as described before [54]. The *antA* upstream region was subdivided into overlapping fragments a-f (100 bp). Each fragment shares a 50 bp overlapping region with its adjacent fragment(s). The fragments were amplified and expanded to 140 bp using oligonucleotides AKHp30-41, which add 20 bp stretches to both sides of the fragment homologous to 5′Cy3-labeled oligonucleotide AKHp28 respectively AKHp29. AKHp28 and AKHp29 were used in a second PCR. EMSAs were performed with minor modifications as described before [54]. Briefly 0.125 pmol 5′-Cy3 labeled DNA fragments, together with 2.5 μg salmon sperm DNA and 0.5 pmol heterologously expressed and purified AntJ were incubated for 5 min at RT in shift buffer [25 mM Tris-acetate, 0.5 mM DTT, 50 mM $KC_2H_3O_2$, 8 mM Mg $(C_2H_3O_2)_2$] before loading on native 4.5% polyacrylamide gels. Protein-DNA complexes were separated from unbound DNA on the gel in TAE buffer (40 mM Tris-acetate pH 7.8, 1 mM EDTA) applying a voltage of 3.5 V/cm. 5′-Cy3 labeled DNA fragments on the gel were detected as described before [54].

4.18. Surface plasmon resonance (SPR) spectroscopy

SPR assays were performed in a Biacore T200 (GE Healthcare, München) using carboxymethyl dextran sensor chips pre-coated with streptavidin (XanTec SAD500L, XanTec Bioanalytics GmbH, Düsseldorf). Biotinylated fragments of the *antA* promoter were generated by amplification of the P_{antA} region using chromosomal DNA of *P. luminescens* as template, and using the biotinylated primer PantA-Btn_fwd and PantA-XmaI_rev. Before immobilizing the DNA fragment, the chip was equilibrated by three injections using 1 M NaCl/50 mM NaOH at a flow rate of 10 μl/min. 10 nM of the respective double-stranded

http://dx.doi.org/10.1016/j.heliyon.2016.e00197

biotinylated DNA fragment was injected using a contact time of 420 s and a flow rate of 10 μl/min. As a final wash step, 1 M NaCl/50 mM NaOH/50% (v/v) isopropanol was injected. Approximately 300 RU of the DNA fragment was captured onto flow cell 2 of the chip. AntJ was diluted in HBS-EP+ buffer [10 mM HEPES, pH 7.4, 150 mM NaCl, 3 mM EDTA, 0.05% (v/v) Surfactant P20] and passed over flow cells 1 and 2 in different concentrations (0 nM, 10 nM, 25 nM, 50 nM, 100 nM, 125 nM, 250 nM, and 500 nM) using a contact time of 180 s followed by a 240 dissociation time before the next cycle started. The experiments were carried out at 25 °C at a flow rate of 30 μl/min. After each cycle the surface was regenerated by injection of 2.5 M NaCl for 60 s at 30 μl/min flow rate. Sensorgrams were recorded using the Biacore T200Control software 2.0 and analyzed with the Biacore T200 Evaluation software 2.0. The surface of flow cell 1 was used to obtain blank sensorgrams for subtraction of bulk refractive index background. The referenced sensorgrams were normalized to a baseline of 0. The 1:1 binding algorithm was used for calculation of the binding affinity. Peaks in the sensorgrams at the beginning and the end of the injection emerged from the runtime difference between the flow cells of each chip. Experiments were performed in the Bioanalytics core facility of the LMU München.

4.19. Phylogenetic analysis

For the identification of the 100 most similar protein sequences of AntJ, a BLASTp search against the non-redundant protein database from NCBI was performed. For the phylogenetic analysis ClustalW was used to align the sequences. Three sequences were deleted from the alignment due to the occurrence of unusual amino acids. The tree was generated with the Geneious tree builder incorporated into Geneious (v6.1.8) (Biomatters Ltd., New Zealand) utilizing the Jukes-Cantor distance model.

Declarations

Author contribution statement

Antje K Heinrich, Angela Glaeser: Conceived and designed the experiments; Performed the experiments; Analyzed and interpreted the data; Wrote the paper.

Nicholas J Tobias, Ralf Heermann, Helge B Bode: Conceived and designed the experiments; Analyzed and interpreted the data; Wrote the paper.

Funding statement

Research in the Bode and the Heermann laboratories were both supported by the Deutsche Forschungsgemeinschaft (SPP1617).

http://dx.doi.org/10.1016/j.heliyon.2016.e00197

Competing interest statement

The authors declare no conflict of interest.

Additional information

Supplementary content related to this article has been published online at http://dx.doi.org/10.1016/j.heliyon.2016.e00197

Acknowledgements

SPR experiments were performed in the Bioanalytics core facility at the LMU Biocenter. We are grateful to Dr. Carsten Kegler for help with the protein pull down assay and to Raphaela Schloßnikel for student assistance.

References

[1] J.-W. Veening, E.J. Stewart, T.W. Berngruber, F. Taddei, O.P. Kuipers, L.W. Hamoen, Bet-hedging and epigenetic inheritance in bacterial cell development, Proc. Natl. Acad. Sci. USA 105 (2008) 4393–4398.

[2] W.K. Smits, C.C. Eschevins, K.A. Susanna, S. Bron, O.P. Kuipers, L.W. Hamoen, Stripping Bacillus: ComK auto-stimulation is responsible for the bistable response in competence development, Mol. Microbiol. 56 (2005) 604–614.

[3] S. Mehra, S. Charaniya, E. Takano, W.-S. Hu, A bistable gene switch for antibiotic biosynthesis: the butyrolactone regulon in *Streptomyces coelicolor*, PLoS ONE 3 (2008) e2724.

[4] J. Grote, D. Krysciak, W.R. Streit, Phenotypic heterogeneity, a phenomenon that may explain why quorum sensing does not always result in truly homogenous cell behavior, Appl. Env. Microbiol. 81 (2015) 5280–5289.

[5] R. Han, R.U. Ehlers, Effect of *Photorhabdus luminescens* phase variants on the in vivo and in vitro development and reproduction of the entomopathogenic nematodes *Heterorhabditis bacteriophora* and *Steinernema carpocapsae*, FEMS Microbiol. Ecol. 35 (2001) 239–247.

[6] R.R. Han, R.U.R. Ehlers, Pathogenicity, Development, and Reproduction of *Heterorhabditis bacteriophora* and *Steinernema carpocapsae* under axenic in vivo conditions, J. Invertebr. Pathol. 75 (2000) 55–58.

[7] D.J. Clarke, *Photorhabdus*: a model for the analysis of pathogenicity and mutualism, Cell. Microbiol. 10 (2008) 2159–2167.

[8] R.H. ffrench-Constant, N. Waterfield, P. Daborn, S. Joyce, H. Bennett, C. Au, et al., *Photorhabdus*: towards a functional genomic analysis of a symbiont and pathogen, FEMS Microbiol. Rev. 26 (2003) 433–456.

[9] R.J. Akhurst, N.E. Boemare, A numerical taxonomic study of the genus *Xenorhabdus* (Enterobacteriaceae) and proposed elevation of subspecies of *X. nematophilus* to species, J. Gen. Microbiol. 134 (1988) 1835–1845.

[10] R.J. Akhurst, Morphological and Functional Dimorphism in *Xenorhabdus* spp, bacteria symbiotically associated with the insect pathogenic nematodes *Neoplectana* and *Heterorhabditis*, J. Gen. Microbiol. 121 (1980) 303–309.

[11] S.A. Joyce, L. Lango, D.J. Clarke, The Regulation of Secondary Metabolism and Mutualism in the Insect Pathogenic Bacterium *Photorhabdus luminescens*, Adv. Appl. Microbiol. 76 (2011) 1–25.

[12] W.H. Richardson, T.M. Schmidt, K.H. Nealson, Identification of an anthraquinone pigment and a hydroxystilbene antibiotic from *Xenorhabdus luminescens*, App. Env. Microbiol. 54 (1988) 1602–1605.

[13] S.A. Joyce, A.O. Brachmann, I. Glazer, L. Lango, G. Schwär, D.J. Clarke, et al., Bacterial biosynthesis of a multipotent stilbene, Angew. Chem. Int. Ed. Engl. 47 (2008) 1942–1945.

[14] A.O. Brachmann, S.A. Joyce, H. Jenke-Kodama, G. Schwär, D.J. Clarke, H. B. Bode, A type II polyketide synthase is responsible for anthraquinone biosynthesis in *Photorhabdus luminescens*, ChemBioChem. 8 (2007) 1721-–1728.

[15] F. Pankewitz, M. Hilker, Polyketides in insects: ecological role of these widespread chemicals and evolutionary aspects of their biogenesis, Biol. Rev. Camb. Philos. Soc. 83 (2008) 209–226.

[16] B. Gulcu, S. Hazir, H.K. Kaya, Scavenger deterrent factor (SDF) from symbiotic bacteria of entomopathogenic nematodes, J. Invertebr. Pathol. 110 (2012) 326–333.

[17] A. Lochowska, R. Iwanicka-Nowicka, D. Plochocka, M.M. Hryniewicz, Functional dissection of the LysR-type CysB transcriptional regulator. Regions important for DNA binding, inducer response, oligomerization, and positive control, J. Biol. Chem. 276 (2001) 2098–2107.

[18] R. Heermann, T.M. Fuchs, Comparative analysis of the *Photorhabdus luminescens* and the *Yersinia enterocolitica* genomes: uncovering candidate genes involved in insect pathogenicity, BMC Genomics 9 (2008) 40.

 http://dx.doi.org/10.1016/j.heliyon.2016.e00197

[19] S. Brameyer, D. Kresovic, H.B. Bode, R. Heermann, LuxR solos in *Photorhabdus* species, Front. Cell. Infect. Microbiol. 4 (166) (2014).

[20] A. Marchler-Bauer, C. Zheng, F. Chitsaz, M.K. Derbyshire, L.Y. Geer, R.C. Geer, et al., CDD: conserved domains and protein three-dimensional structure, Nucleic Acids Res. 41 (2013) D348–352.

[21] N.J. Tobias, B. Mishra, D.K. Gupta, R. Sharma, M. Thines, T.P. Stinear, et al., Genome comparisons provide insights into the role of secondary metabolites in the pathogenic phase of the *Photorhabdus* life cycle, BMC Genomics 17 (537) (2016).

[22] H.B. Bode, D. Reimer, S.W. Fuchs, F. Kirchner, C. Dauth, C. Kegler, et al., Determination of the absolute configuration of peptide natural products by using stable isotope labeling and mass spectrometry, Chemistry 18 (2012) 2342–2348.

[23] A.O. Brachmann, S. Brameyer, D. Kresovic, I. Hitkova, Y. Kopp, C. Manske, et al., Pyrones as bacterial signaling molecules, Nat. Chem. Biol. 9 (2013) 573–578.

[24] F.I. Nollmann, A.K. Heinrich, A.O. Brachmann, C. Morisseau, K. Mukherjee, Á.M. Casanova-Torres, et al., A *Photorhabdus* natural product inhibits insect juvenile hormone epoxide hydrolase, ChemBioChem. 16 (2015) 766–771.

[25] A. Glaeser, R. Heermann, A novel tool for stable genomic reporter gene integration to analyze heterogeneity in *Photorhabdus luminescens* at the single-cell level, Biotech. 59 (2015) 74–81.

[26] S. Behr, R. Heermann, K. Jung, Insights into the DNA-binding mechanism of a LytTR-type transcription regulator, Biosci. Rep. 36 (2016) e00326.

[27] A. Chastanet, D. Vitkup, G.-C. Yuan, T.M. Norman, J.S. Liu, R.M. Losick, Broadly heterogeneous activation of the master regulator for sporulation in *Bacillus subtilis*, Proc. Natl. Acad. Sci. USA 107 (2010) 8486–8491.

[28] L. Plener, N. Lorenz, M. Reiger, T. Ramalho, U. Gerland, K. Jung, The Phosphorylation Flow of the *Vibrio harveyi* Quorum-Sensing Cascade Determines Levels of Phenotypic Heterogeneity in the Population, J. Bacteriol. 197 (2015) 1747–1756.

[29] S.A. Joyce, D.J. Clarke, A *hexA* homologue from *Photorhabdus luminescens* regulates pathogenicity, symbiosis and phenotypic variation, Mol. Microbiol. 47 (5) (2003) 1445–1457.

 http://dx.doi.org/10.1016/j.heliyon.2016.e00197

[30] R. Kontnik, J.M. Crawford, J. Clardy, Exploiting a Global Regulator for Small Molecule Discovery in *Photorhabdus luminescens*, ACS Chem. Biol. 5 (2010) 659–665.

[31] C.A. Easom, D.J. Clarke, HdfR is a regulator in *Photorhabdus luminescens* that modulates metabolism and symbiosis with the nematode *Heterorhabditis*, Environ. Microbiol. 14 (2012) 953–966.

[32] M. Stalman, A.-M. Koskamp, R. Luderer, J.H. Vernooy, J.C. Wind, G.J. Wullems, et al., Regulation of anthraquinone biosynthesis in cell cultures of *Morinda citrifolia*, J. Plant Physiol. 160 (2003) 607–614.

[33] F.Y. Lim, Y. Hou, Y. Chen, J.-H. Oh, I. Lee, T.S. Bugni, et al., Genome-based cluster deletion reveals an endocrocin biosynthetic pathway in *Aspergillus fumigatus*, Appl. Env. Microbiol. 78 (2012) 4117–4125.

[34] M.B. Elowitz, A.J. Levine, E.D. Siggia, P.S. Swain, Stochastic gene expression in a single cell, Science 297 (2002) 1183–1186.

[35] M. Ackermann, A functional perspective on phenotypic heterogeneity in microorganisms, Nat. Rev. Micro. 13 (2015) 497–508.

[36] W.J. Blake, M. KAErn, C.R. Cantor, J.J. Collins, Noise in eukaryotic gene expression, Nature 422 (2003) 633–637.

[37] D. Huh, J. Paulsson, Non-genetic heterogeneity from stochastic partitioning at cell division, Nat. Genet. 43 (2011) 95–100.

[38] S.V. Avery, Microbial cell individuality and the underlying sources of heterogeneity, Nat. Rev. Micro. 4 (2006) 577–587.

[39] K. Miller-Jensen, S.S. Dey, D.V. Schaffer, A.P. Arkin, Varying virulence: epigenetic control of expression noise and disease processes, Trends Biotechnol. 29 (2011) 517–525.

[40] H.B. Bode, A.O. Brachmann, K.B. Jadhav, L. Seyfarth, C. Dauth, S.W. Fuchs, et al., Structure Elucidation and Activity of Kolossin A, the D-/L-Pentadecapeptide Product of a Giant Nonribosomal Peptide Synthetase, Angew. Chem. Int. Ed. Engl. 54 (2015) 10352–10355.

[41] J. Sambrook, E.F. Fritsch, T. Maniatis, Molecular Cloning: A Laboratory Manual, 2nd ed., Cold Spring Harbor Laboratory Press, New York, 1989.

[42] S. Thoma, M. Schobert, An improved *Escherichia coli* donor strain for diparental mating, FEMS Microbiol. Lett. 294 (2009) 127–132.

[43] H. Inoue, H. Nojima, H. Okayama, High efficiency transformation of *Escherichia coli* with plasmids, Gene 96 (1990) 23–28.

 http://dx.doi.org/10.1016/j.heliyon.2016.e00197

[44] N. Philippe, J.-P. Alcaraz, E. Coursange, J. Geiselmann, D. Schneider, Improvement of pCVD442, a suicide plasmid for gene allele exchange in bacteria, Plasmid 51 (2004) 246–255.

[45] D. Wessel, U.I. Flügge, A method for the quantitative recovery of protein in dilute solution in the presence of detergents and lipids, Anal. Biochem. 138 (1984) 141–143.

[46] A. Shevchenko, H. Tomas, J. Havlis, J.V. Olsen, M. Mann, In-gel digestion for mass spectrometric characterization of proteins and proteomes, Nat. Protoc. 1 (2006) 2856–2860.

[47] S.W. Fuchs, K.A.J. Bozhüyük, D. Kresovic, F. Grundmann, V. Dill, A.O. Brachmann, et al., Formation of 3-cyclohexanediones and resorcinols catalyzed by a widely occurring ketosynthase, Angew. Chem. Int. Ed. Engl. 52 (2013) 4108–4112.

[48] K.J. Livak, T.D. Schmittgen, Analysis of relative gene expression data using real-time quantitative PCR and the 2(-Delta Delta C(T)) Method, Methods 25 (2001) 402–408.

[49] E. Duchaud, C. Rusniok, L. Frangeul, C. Buchrieser, A. Givaudan, S. Taourit, et al., The genome sequence of the entomopathogenic bacterium *Photorhabdus luminescens*, Nat. Biotechnol. 21 (2003) 1307–1313.

[50] D. Reimer, K.M. Pos, M. Thines, P. Grün, H.B. Bode, A natural prodrug activation mechanism in nonribosomal peptide synthesis, Nat. Chem. Biol. 7 (2011) 888–890.

[51] R. Heermann, K. Altendorf, K. Jung, The N-terminal input domain of the sensor kinase KdpD of *Escherichia coli* stabilizes the interaction between the cognate response regulator KdpE and the corresponding DNA-binding site, J. Biol. Chem. 278 (2003) 51277–51284.

[52] F.W. Studier, Protein production by auto-induction in high density shaking cultures, Protein Expr. Purif. 41 (2005) 207–234.

[53] T.A. Schöner, S.W. Fuchs, C. Schönau, H.B. Bode, Initiation of the flexirubin biosynthesis in *Chitinophaga pinensis*, Microb. Biotechnol. 7 (2014) 232–241.

[54] C. Volz, C. Kegler, R. Müller, Enhancer binding proteins act as hetero-oligomers and link secondary metabolite production to myxococcal development, motility, and predation, Chem. Biol. 19 (2012) 1447–1459.

[55] T.D. Schmittgen, K.J. Livak, Analyzing real-time PCR data by the comparative C(T) method, Nat. Protoc. 3 (2008) 1101–1108.

 http://dx.doi.org/10.1016/j.heliyon.2016.e00197